GA–A26434

DESCRIPTION AND PRELIMINARY RESULTS OF A NEW PHOTO DETECTOR FOR THE DIII-D THOMSON SCATTERING DIAGNOSTIC

by
T.M. DETERLY, B.D. BRAY, C.-L. HSIEH, J.A. KULCHAR, C. LIU, and D.M. PONCE

JUNE 2009

GENERAL ATOMICS

DISCLAIMER

GA–A26434

DESCRIPTION AND PRELIMINARY RESULTS OF A NEW PHOTO DETECTOR FOR THE DIII-D THOMSON SCATTERING DIAGNOSTIC

by
T.M. DETERLY, B.D. BRAY, C.-L. HSIEH, J.A. KULCHAR, C. LIU, and D.M. PONCE

This is a preprint of an invited paper to be presented at the Twenty-Third Symposium on Fusion Engineering, May 31 through June 5, 2009, San Diego, California, and to be published in the *Proceedings.*

Work supported in part by
the U.S. Department of Energy
under DE-FC02-04ER54698

GENERAL ATOMICS PROJECT 30200
JUNE 2009

Description and Preliminary Results of a New Photo Detector for the DIII-D Thomson Scattering Diagnostic

T.M. Deterley, B.D. Bray, C.-L. Hsieh, J.A. Kulchar, C. Liu, and D.M. Ponce
General Atomics
PO Box 85608
San Diego, California 92186-5608
deterly@fusion.gat.com

***Abstract*— A redesign of the Thomson scattering data acquisition system located on the DIII-D tokamak is undergoing its trial phase. The redesign was made necessary by several factors including the desire to improve the quality of the acquired data. In addition, the previous generation system was based on CAMAC technology, which has become difficult to maintain and is no longer supported. A big part of this improved redesign comes from the use of faster electronics allowing for greatly improved background light subtraction, the main source of noise. The past system utilized LeCroy FERA CAMAC gated integrator modules for integration and digitization. The redesigned system has been designed in a much more distributed manner. The new system consists of a number of subsystems, including: photo detectors, digitizers, distribution panels, and timing circuits. The most significant upgrade was performed on the photo detectors electronics assembly. A key feature was to make the units much more self-contained in regards to the preamplifier, background subtraction, integration, and bias circuits. The redesigned photo detectors and preliminary test results of the trial phase will be presented.**

Keywords-data acquisition; photo detector; Thomson scattering

I. OVERVIEW

A new data acquisition (DAQ) system for the Thomson scattering diagnostic on the DIII-D tokamak has undergone its evaluation period. The newly designed system has been implemented primarily to improve the diagnostic's data quality and to modernize aging hardware. The previous system has been evolving since the late 1980's [1], but hasn't undergone a complete redesign until now. During this time period new higher speed lower noise technology has become available that is capable of significantly improving both the measurement quality as well as simplifying the system. This technology has warranted the design and implementation of the new Thomson scattering DAQ system.

The new system consists of a number of subsystems including photo detectors, digitizers, timing and signal distribution and system control. An overview of the complete Thomson scattering system including the DAQ system is shown in Fig. 1. A critical part of the system is the design of the photo detectors. This design was guided by a number of constraints dictated by the desired specifications of Thomson scattering diagnostic as implemented on DIII-D. These constraints include: low light levels (100's of photons) [2] visible to near infrared wavelengths (700 to 1060 nm, Nd:YAG lasers), short pulse widths (8 to 12 ns), high repetition rates (100 kHz), high background light levels, high channel count and constrained physical size.

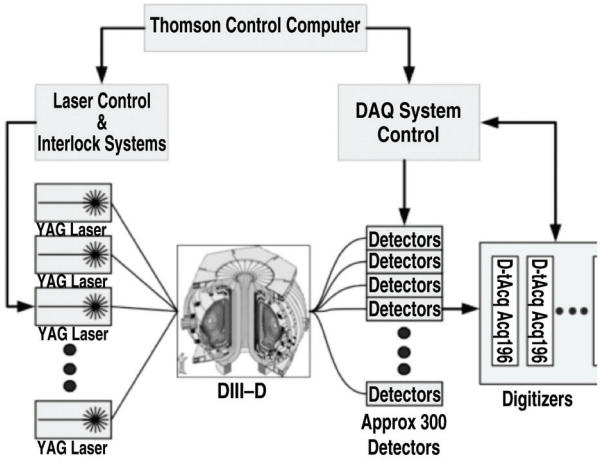

Figure 1. Thomson scattering system overview.

To meet these constraints the photo detectors were designed using an avalanche photo diode (APD) as the transducer, a new preamplifier circuit, background subtraction circuit, gated integrator, and sample and hold (S/H) circuits. The key design differences between the new detector and the previous detector's design include a much higher bandwidth preamplifier, faster background subtraction and the incorporation of the gated integrator and S/H circuits in the detectors. The design of this detector and the preliminary system results are discussed in this paper.

II. PHOTO DETECTOR DESIGN

As with most second generation designs the design of this detector leveraged off the experience gained from the first generation design [3]. The basic circuit architecture of the previous design can still be seen in the new design, but lower levels have all been redesigned. A block diagram of the new photo detector can be seen Fig. 2. As shown, the detector consists of a number of subsections which will be discussed below.

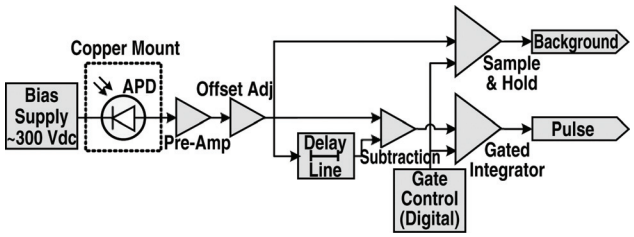

Figure 2. Photo detector block diagram.

A. Front End

The detectors front end is a near infrared (NIR) enhanced APD. It was decided that the new system would use the same APDs as the previous system did due to the cost of purchasing new APDs along with the fact only modest improvements in NIR APD technologies have occurred. Even though the APD didn't change, its bias supply and the control of its thermal stabilization have.

In the previous system design, there was one centralized high voltage bias supply that was divided down to give a fixed number of different voltage settings for the APDs. With the new system each detector gets its own internal high voltage supply which is continuously variable up to 500 Vdc. This provides two major improvements: it allows each APD to be set to the exact voltage/gain desired and also makes the system safer, having low current supplies as opposed to a much higher current supply that also requires a method of distribution.

The thermal properties of the detector with regards to the APD temperature stabilization have also been improved. In the previous design it was found that temperature variations in the temperature controlled room caused the APDs temperature to drift which would change the gain of the detectors. To circumvent this issue the new detector design surrounds the APD with a copper-based socket that attaches to the water cooled polychromators. This arrangement keeps the APD temperature much more stable. In addition to this stabilization, a thermistor and associated circuit was added to the detector to monitor the APD temperature and allow software based temperature compensation.

B. Preamplifier

Directly following the APD is a newly designed high bandwidth low noise transimpedance preamplifier circuit. The particular op-amp chosen, National Semiconductor's LMH6624, was selected for its very low input noise levels along with its equally high bandwidth. The requirements for both low noise and high bandwidth are dictated by the optical properties of the Thomson system; the typical pulse width of the YAG lasers is 8 ns and the amount of light seen by the detectors can be less than 100 photons.

In the previous design it was thought that having a lower bandwidth detector would be beneficial with regards to signal to noise ratio (S/N). However, since then, further models have been developed which have shown this not the case and that higher bandwidth detection should provide a better S/N ratio. The increased S/N ratio comes from the fact that with a shorter apparent pulse width the integration gate can also be shortened. By shorting the integration gate the noise component from the background signal has less time to accumulate and, therefore, its contribution to the final result is less significant. A comparison between the preamplifier outputs of the new detector design and the previous design can be seen in Fig. 3. As shown, with the new design the pulse width after detection is approximately 25 ns, whereas with the previous detector response the same pulse is about 200 ns.

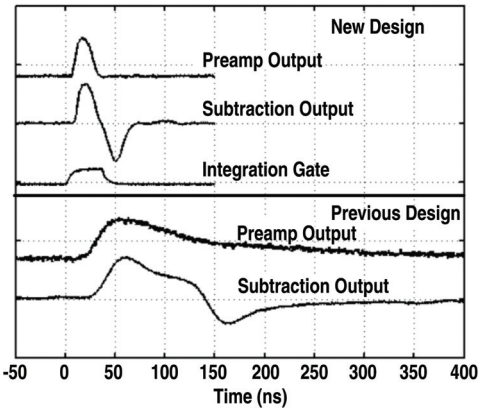

Figure 3. Pulse signal comparison.

C. Background Subtraction

Following the preamplifier and an offset adjustment circuit the signal is split into two separate paths. One path leads to the S/H amplifier which captures the background light to be used later in determining the quality of the measurement. The other path is sent to the background subtraction circuit which in turn feeds the integrator, leading to the primary output.

The background subtraction circuit is critical to the entire measurement due to the very high levels of background light seen relative to the desired pulse light. The method chosen to remove the background light is based on typical subtraction circuit with the addition of a delay line. By utilizing the delay line the subtraction circuit subtracts the current signal from the past signal. So, as the pulse signal moves through the subtraction circuit the background signal, coming from the delay line, is removed. Due to variations in the delay lines a potentiometer is used to scale the amount of background signal that is subtracted.

For this new design the delay line was chosen to have a delay of 30 ns. The delay was chosen based on the pulse width seen after the preamplifier. Ideally the delay should be as short as possible allowing the background light levels the least

amount of time to fluctuate. However if the delay is shorter than the signal's pulse width, the subtraction circuit ends up subtracting parts the signal of interest. As shown in Fig. 3, the delay of 30 ns gives just enough time for the pulse to be isolated from its subtracted counterpart.

D. Integrator and Sample and Hold

After background subtraction, the pulse signal is sent to a differential integrator, and the composite signal coming from the preamplifier is sent to an S/H circuit. From there the signals are buffered and sent out to be digitized.

The requirements of both the integrator and S/H circuits are very demanding. Both require precision low noise analog circuitry coupled with high speed digital switching. In the case of the integrator, the integration capacitors must be enabled and disabled with a gating width of 30 ns, without allowing the switching mechanism to interfere with the signal being integrated. In addition, the switching must not affect the leakage rates of the storage capacitors in both the S/H circuit as well as the integrator. Due to these requirements, a number of different switch technologies were evaluated along with different integrator architectures.

A number of different switches were evaluated with emphasis on low charge injection, fast turn on and off times, bandwidth, leakage, and drive requirements with the final choice being an ultra high speed CMOS analog switch (Fairchild FSA66). The advantage of this type of switch, over a discrete switch, is that it doesn't require a specialized drive circuitry. However, they are typically designed for single supply operation, where for the photo detector a dual supply is required. To deal with this issue the switches in both the integrator and the S/H circuits are floated between -2.5 V and +2.5 V. By shifting the switches down to -2.5 V it allows the negative signal from the subtraction circuit to pass into the integrator unaffected. A consequence of this is that the switch control also be shifted down to -2.5 V. The control signals are shifted down by a passive resistor divider circuit, shown in Fig. 4.

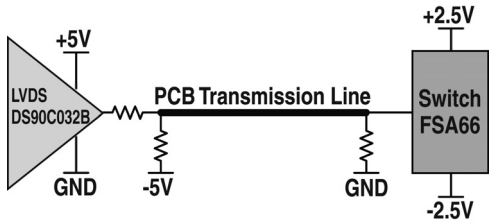

Figure 4. Analog switch control.

In addition to evaluating different analog switches, different integrator designs were investigated. Due to the system's pulse width and the lack of an ideal switch, a differential integrator was chosen. By using a differential integrator the effect of charge injection caused by the analog switches is greatly reduced. Along with the charge injection, the effects of the on and off resistances seen in the analog switches is also reduced.

III. RESULTS

For the trial, it was decided we would convert the diverter section of the Thomson system over to the new design. The diverter section consists of eight different polychromators (viewing channels), each of which are sampled by five detectors giving a total of 40 detectors.

The first stage after receiving the detectors from the contract manufacture is to perform electrical calibration and install the APDs. This involves setting the APD bias voltage to a pre-calculated value based on the particular APD specification sheet. Then the calibration of the preamplifier must be preformed. This calibration is done by using a pulsed laser source and adjusting the feedback capacitance of the preamplifier to minimize oscillations while maximizing gain. After the preamplifier is calibrated the offset adjustment can be adjusted by blocking all light to the detector. Finally the subtraction circuit is calibrated by using both pulsed and CW lasers and adjusting the output of to have a zero bias on the pulse channel.

Following the electrical calibration, each detector is optically calibrated. During this calibration the data from each detector is digitized over four different intensities of CW laser light and four different amplitudes of pulsed laser light. By performing these scans a pretty comprehensive data set showing the performance of each detector is obtained. One important statistic that comes from this data set is the standard deviation (STD) of the pulse channel in presence of increasing background light. This statistic is of high importance due to the very high background light levels, which are the main contributor of noise for the Thomson diagnostic. Figure 5 shows a comparison between the new detector design and the previous detector design based on this calibration. It can be seen that the pulse channel noise from the new design is significantly improved compared to that of the previous design. In addition the linearity of the noise is also improved which helps with estimating the system errors.

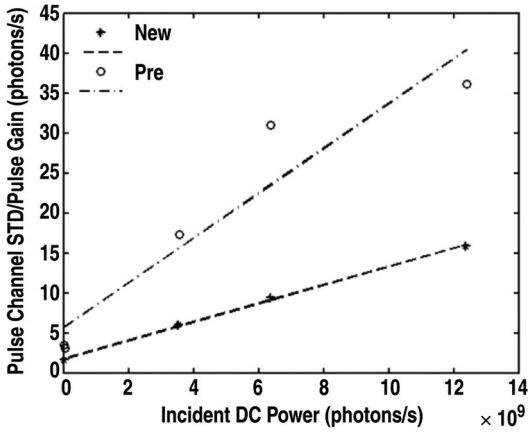

Figure 5. Pulse channel noise comparison at 1064nm

The final system calibratio n is Rayleigh scattering. This calibration tests and calibrates the entire Thomson scattering diagnostic. It involves filling the DIII-D vessel with four or

more different pressure levels of argon gas and taking scattering data at each level. Typically this pressure scan is preformed at least twice. As with the other calibrations the results are used for both calibration purposes as well as a means to evaluate the system. For evaluation use the data is looked at to ensure that each pressure level can be distinguished from the other pressure levels, that the values of both runs agree, and that the recorded values increase with increasing pressure. The results from both the new system as well as the previous system are shown in Fig. 6. As Fig. 6 shows the new design is greatly improved in all aspects; separation, linearity, stray light rejection, and repeatability, compared to the previous design. The improvement in separation, the ability to clearly distinguish between adjacent pressure levels, is due to both the increased gain of the new system as well as the lower noise levels.

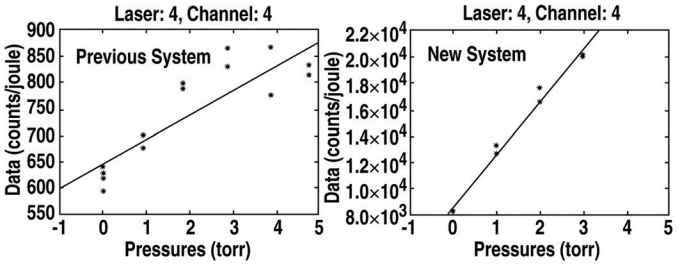

Figure 6. Rayleigh scattering comparison.

Following Rayleigh scattering, the detectors ran during regular DIII-D operations. During this period a plasma discharge was preformed with matching physical parameters from a year past in order to compare the new design with the previous design. The results from this discharge showed that the signal to noise (S/N) ratio in both low background and high background light levels were significantly improved. An example of this data, taken from two channels of one of the eight polychromators, is shown in Fig. 7. The 1047 nm filter is a narrowband filter causing low background light levels, where the 1005 nm is a broader band filter allowing high background light levels. As shown the S/N ratio for the low background levels has a six times improvement and in the case of the high background levels a two and a half times increase.

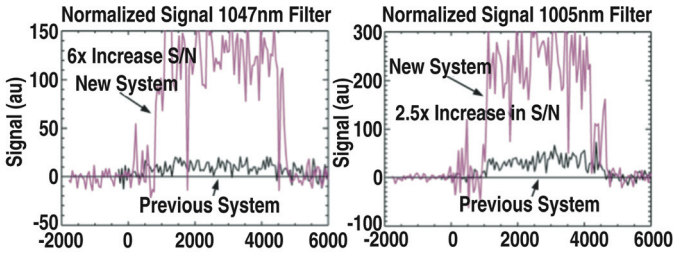

Figure 7. Plasma comparison.

IV. CONCLUSIONS

The design of the new DAQ system has undergone a number of different calibration and evaluation procedures, including being installed on the diverter section of the DIII-D Thomson scattering diagnostic. During this time the system has proven to be reliable, and provide high quality temperature and density data.

The reliability of the system has been excellent. Out of the fifty detectors manufactured only two did not make it through the calibration procedures and only one has failed since. Besides the detectors, the new distribution system and digitizers have also proved to be very reliable. The new system, as a whole, has had very few issues since it went online in January 2009.

In addition to the system's reliability, the quality of the data produced has also been excellent. The new design has allowed new measurements to be made that previously were not possible due to the noise levels. The system has increased the signal to noise ratio on average by a factor of four.

Based on this trial period and the results outlined in this paper it has been decided to continue with the upgrade and convert the remaining sections of the Thomson system to the new design.

ACKNOWLEDGMENT

This work was supported by the US Department of Energy under DE-FC02-04ER54698.

REFERENCES

[1] C-L. Hsieh, J. Haskovec, T.N. Carlstrom, J. C. Deboo, C.M. Greenfield, R.T. Snider, and P. Trost, Rev. Sci. Instrum. **61**, 2857 (1990).

[2] C.M. Greenfield, G.L. Campbell, T.N.Carlstrom, J.C. DeBoo, C.-L. Hsieh, R.T. Snider, and P.K. Trost, Rev. Sci. Instrum. **61**, 3288 (1990).

[3] T.N. Carlstrom, G.L. Campbell, J.C. Deboo, R. Evanko, J. Evans, C.M. Greenfield, J. Haskovec, C.L. Hsieh, E. McKee, R.T. Snider, R. Stockdale, P.K. Trost, and M.P. Thomas, Rev. Sci. Instrum. **63**, 4906 (1992).